

Inductive Bias of Deep Convolutional Networks through Pooling Geometry

Nadav Cohen
The Hebrew University of Jerusalem
cohennadav@cs.huji.ac.il

Amnon Shashua
The Hebrew University of Jerusalem
shashua@cs.huji.ac.il

Abstract

Our formal understanding of the inductive bias that drives the success of convolutional networks on computer vision tasks is limited. In particular, it is unclear what makes hypotheses spaces born from convolution and pooling operations so suitable for natural images. In this paper we study the ability of convolutional arithmetic circuits to model correlations among regions of their input. Correlations are formalized through the notion of separation rank, which for a given input partition, measures how far a function is from being separable. We show that a polynomially sized deep network supports exponentially high separation ranks for certain input partitions, while being limited to polynomial separation ranks for others. The network's pooling geometry effectively determines which input partitions are favored, thus serves as a means for controlling the inductive bias. Contiguous pooling windows as commonly employed in practice favor interleaved partitions over coarse ones, orienting the inductive bias towards the statistics of natural images. In addition to analyzing deep networks, we show that shallow ones support only linear separation ranks, and by this gain insight into the benefit of functions brought forth by depth – they are able to efficiently model strong correlation under favored partitions of the input.

1 Introduction

A central factor in the application of machine learning to a given task is the *inductive bias*, i.e. the choice of hypotheses space from which learned functions are taken. The restriction posed by the inductive bias is necessary for practical learning, and reflects prior knowledge regarding the task at hand. Perhaps the most successful exemplar of inductive bias to date manifests itself in the use of convolutional networks ([18]) for computer vision tasks. These hypotheses spaces are delivering unprecedented visual recognition results (e.g. [17, 27, 26, 14]), largely responsible for the resurgence of deep learning ([19]). Unfortunately, our formal understanding of the inductive bias behind convolutional networks is limited – the assumptions encoded into these models, which seem to form an excellent prior knowledge for imagery data, are for the most part a mystery.

Existing works studying the inductive bias of deep networks (not necessarily convolutional) do so in the context of *depth efficiency*, essentially arguing that for a given amount of resources, more layers result in higher expressiveness. More precisely, depth efficiency refers to a situation where a function realized by a deep network of polynomial size, requires exponential size in order to be realized (or approximated) by a shallower network. In recent years, a large body of research was devoted to proving existence of depth efficiency under different types of architectures (see for example [9, 23, 21, 28, 10, 24, 20]). Nonetheless, despite the wide attention it is receiving, depth efficiency does not convey the complete story behind the inductive bias of deep networks. While it does suggest that depth brings forth functions that are otherwise unattainable, it does not explain why these functions are useful. Loosely speaking, the hypotheses space of a polynomially sized deep

network covers a small fraction of the space of all functions. We would like to understand why this small fraction is so successful in practice.

A specific family of convolutional networks gaining increased attention is that of *convolutional arithmetic circuits*. These models follow the standard paradigm of locality, weight sharing and pooling, yet differ from the most conventional convolutional networks in that their point-wise activations are linear, with non-linearity originating from product pooling. Recently, [8] analyzed the depth efficiency of convolutional arithmetic circuits, showing that besides a negligible set, all functions realizable by a deep network require exponential size in order to be realized (or approximated) by a shallow one. This result, termed *complete depth efficiency*, stands in contrast to previous results along this line, which merely showed *existence* of functions efficiently realizable by deep networks but not by shallow ones. In subsequent work, [6] proved that for the popular convolutional rectifier networks, *i.e.* convolutional networks with rectified linear (ReLU, [22]) activation and max or average pooling, depth efficiency exists but it is not complete, meaning such networks are inferior to convolutional arithmetic circuits in terms of depth efficiency. Motivated by these results, and by the fact that convolutional arithmetic circuits are equivalent to SimNets, a new deep learning architecture that has recently demonstrated promising empirical performance ([5, 7]), we focus in this paper on convolutional arithmetic circuits as representatives of the class of convolutional networks.

We approach the study of inductive bias from the direction of function inputs. Specifically, we study the ability of convolutional arithmetic circuits to model correlation between regions of their input. To analyze the correlations of a function, we consider different partitions of input regions into disjoint sets, and ask how separable the function is w.r.t. these partitions. Separability of a function w.r.t. a partition of its input is measured through the notion of *separation rank* ([2]), which can be viewed as quantifying how far the function is from being equal to a product of factors, each depending on input regions from only one side of the partition. High separation rank (low separability) implies that the function induces strong correlation between sides of the partition, and vice versa.

Our analysis shows that a polynomially sized deep network supports exponentially high separation ranks for certain input partitions, while being limited to polynomial or linear (in network size) separation ranks for others. The network’s pooling geometry effectively determines which input partitions are favored in terms of separation rank, *i.e.* which partitions enjoy exponentially high separation ranks with polynomially sized networks, and which require networks to be exponentially large. With the standard choice of square contiguous pooling windows, interleaved (entangled) partitions are favored over coarse ones that divide the input into large distinct areas. We thus conclude that in terms of modeled correlations, pooling geometry controls the inductive bias, and the particular design commonly employed in practice orients it towards the statistics of natural images (nearby pixels more correlated than distant ones).

With regards to depth efficiency, we show that separation ranks under favored input partitions are exponentially high for all but a negligible set of functions realizable by a deep network. Shallow networks on the other hand, treat all partitions equally and support only linear (in network size) separation ranks. Therefore, almost all functions that may be realized by a deep network require a replicating shallow network to have exponential size. By this we return to the complete depth efficiency result of [8], but with an added important insight into the benefit of functions brought forth by depth – they are able to efficiently model strong correlation under favored partitions of the input.

The remainder of the paper is organized as follows. Sec. 2 provides a brief presentation of necessary background material from the field of tensor analysis. Sec. 3 describes the convolutional arithmetic circuits we analyze, and their relation to tensor decompositions. In sec. 4 we convey the concept of separation rank, on which we base our analyses in sec. 5 and 6. Finally, sec. 7 concludes.

2 Preliminaries

The analyses carried out in this paper rely on concepts and results from the field of tensor analysis. In this section we establish the minimal background required in order to follow our arguments ¹, referring the interested reader to [12] for a broad and comprehensive introduction to the field.

¹ The definitions we give are actually concrete special cases of more abstract algebraic definitions as given in [12]. We limit the discussion to these special cases since they suffice for our needs and are easier to grasp.

The core concept in tensor analysis is a *tensor*, which for our purposes may simply be thought of as a multi-dimensional array. The *order* of a tensor is defined to be the number of indexing entries in the array, which are referred to as *modes*. The *dimension* of a tensor in a particular mode is defined as the number of values that may be taken by the index in that mode. For example, a 4-by-3 matrix is a tensor of order 2, *i.e.* it has two modes, with dimension 4 in mode 1 and dimension 3 in mode 2. If \mathcal{A} is a tensor of order N and dimension M_i in each mode $i \in [N] := \{1, \dots, N\}$, the space of all configurations it can take is denoted, quite naturally, by $\mathbb{R}^{M_1 \times \dots \times M_N}$.

A fundamental operator in tensor analysis is the *tensor product*, which we denote by \otimes . It is an operator that intakes two tensors $\mathcal{A} \in \mathbb{R}^{M_1 \times \dots \times M_P}$ and $\mathcal{B} \in \mathbb{R}^{M_{P+1} \times \dots \times M_{P+Q}}$ (orders P and Q respectively), and returns a tensor $\mathcal{A} \otimes \mathcal{B} \in \mathbb{R}^{M_1 \times \dots \times M_{P+Q}}$ (order $P+Q$) defined by: $(\mathcal{A} \otimes \mathcal{B})_{d_1, \dots, d_{P+Q}} = \mathcal{A}_{d_1, \dots, d_P} \cdot \mathcal{B}_{d_{P+1}, \dots, d_{P+Q}}$. Notice that in the case $P = Q = 1$, the tensor product reduces to the standard outer product between vectors, *i.e.* if $\mathbf{u} \in \mathbb{R}^{M_1}$ and $\mathbf{v} \in \mathbb{R}^{M_2}$, then $\mathbf{u} \otimes \mathbf{v}$ is no other than the rank-1 matrix $\mathbf{u}\mathbf{v}^\top \in \mathbb{R}^{M_1 \times M_2}$.

We now introduce the important concept of *matricization*, which is essentially the rearrangement of a tensor as a matrix. Suppose \mathcal{A} is a tensor of order N and dimension M_i in each mode $i \in [N]$, and let (I, J) be a partition of $[N]$, *i.e.* I and J are disjoint subsets of $[N]$ whose union gives $[N]$. We may write $I = \{i_1, \dots, i_{|I|}\}$ where $i_1 < \dots < i_{|I|}$, and similarly $J = \{j_1, \dots, j_{|J|}\}$ where $j_1 < \dots < j_{|J|}$. The *matricization of \mathcal{A} w.r.t. the partition (I, J)* , denoted $[\mathcal{A}]_{I, J}$, is the $\prod_{t=1}^{|I|} M_{i_t}$ -by- $\prod_{t=1}^{|J|} M_{j_t}$ matrix holding the entries of \mathcal{A} such that $\mathcal{A}_{d_1, \dots, d_N}$ is placed in row index $1 + \sum_{t=1}^{|I|} (d_{i_t} - 1) \prod_{t'=t+1}^{|I|} M_{i_{t'}}$ and column index $1 + \sum_{t=1}^{|J|} (d_{j_t} - 1) \prod_{t'=t+1}^{|J|} M_{j_{t'}}$. If $I = \emptyset$ or $J = \emptyset$, then by definition $[\mathcal{A}]_{I, J}$ is a row or column (respectively) vector of dimension $\prod_{t=1}^N M_t$ holding $\mathcal{A}_{d_1, \dots, d_N}$ in entry $1 + \sum_{t=1}^N (d_t - 1) \prod_{t'=t+1}^N M_{t'}$.

A well known matrix operator is the *Kronecker product*, which we denote by \odot . For two matrices $A \in \mathbb{R}^{M_1 \times M_2}$ and $B \in \mathbb{R}^{N_1 \times N_2}$, $A \odot B$ is the matrix in $\mathbb{R}^{M_1 N_1 \times M_2 N_2}$ holding $A_{ij} B_{kl}$ in row index $(i-1)N_1 + k$ and column index $(j-1)N_2 + l$. Let \mathcal{A} and \mathcal{B} be tensors of orders P and Q respectively, and let (I, J) be a partition of $[P+Q]$. The basic relation that binds together the tensor product, the matricization operator, and the Kronecker product, is:

$$[\mathcal{A} \otimes \mathcal{B}]_{I, J} = [\mathcal{A}]_{I \cap [P], J \cap [P]} \odot [\mathcal{B}]_{(I-P) \cap [Q], (J-P) \cap [Q]} \quad (1)$$

where $I - P$ and $J - P$ are simply the sets obtained by subtracting P from each of the elements in I and J respectively. In words, eq. 1 implies that the matricization of the tensor product between \mathcal{A} and \mathcal{B} w.r.t. the partition (I, J) of $[P+Q]$, is equal to the Kronecker product between two matricizations: that of \mathcal{A} w.r.t. the partition of $[P]$ induced by the lower values of (I, J) , and that of \mathcal{B} w.r.t. the partition of $[Q]$ induced by the higher values of (I, J) .

3 Convolutional arithmetic circuits

The convolutional arithmetic circuit architecture on which we focus in this paper is the one considered in [8], portrayed in fig. 1(a). Instances processed by a network are represented as N -length sequences of s -dimensional vectors. They are generally thought of as images, with the s -dimensional vectors corresponding to local patches. For example, instances could be 32-by-32 RGB images, with local patches being 5×5 regions crossing the three color bands. In this case, assuming a patch is taken around every pixel in an image (boundaries padded), we have $N = 1024$ and $s = 75$. Throughout the paper, we denote a general instance by $X = (\mathbf{x}_1, \dots, \mathbf{x}_N)$, with $\mathbf{x}_i \in \mathbb{R}^s$ standing for its patches.

The first layer processing an instance is referred to as *representation*. It consists of applying M *representation functions* $f_{\theta_1} \dots f_{\theta_M} : \mathbb{R}^s \rightarrow \mathbb{R}$ to all patches, thereby creating M feature maps. In the case where representation functions are chosen as $f_{\theta_d}(\mathbf{x}) = \sigma(\mathbf{w}_d^\top \mathbf{x} + b_d)$, with parameters $\theta_d = (\mathbf{w}_d, b_d) \in \mathbb{R}^s \times \mathbb{R}$ and some point-wise activation $\sigma(\cdot)$, the representation layer reduces to a standard convolutional layer. More elaborate settings are also possible, for example modeling the representation as a cascade of convolutional layers with pooling in-between. Following the representation, a network includes L hidden layers indexed by $l = 0 \dots L-1$. Each hidden layer l begins with a 1×1 *conv* operator, which is simply a three-dimensional convolution with r_l channels and 1×1 filter spatiality. This is followed by spatial pooling, that decimates feature maps by taking products of non-overlapping two-dimensional windows that cover the spatial extent. The last of the L hidden layers ($l = L-1$) reduces feature maps to singletons (its pooling operator is global), creating

a vector of dimension r_{L-1} . This vector is mapped into Y network outputs through a final dense linear layer.

Altogether, the architectural parameters of a network are the type of representation functions (f_{θ_d}), the pooling window shapes and sizes (which in turn determine the number of hidden layers L), and the number of channels in each layer (M for representation, $r_0 \dots r_{L-1}$ for hidden layers, Y for output). Given these architectural parameters, the learnable parameters of a network are the representation weights (θ_d for channel d), the conv weights ($\mathbf{a}^{l,\gamma}$ for channel γ of hidden layer l), and the output weights ($\mathbf{a}^{L,y}$ for output node y).

For a particular setting of weights, every node (neuron) in a given network realizes a function from $(\mathbb{R}^s)^N$ to \mathbb{R} . The *receptive field* of a node refers to the indexes of input patches on which its function may depend. For example, the receptive field of node j in channel γ of conv operator at hidden layer 0 is $\{j\}$, and that of an output node is $[N]$, corresponding to the entire input. Denote by $h_{(l,\gamma,j)}$ the function realized by node j of channel γ in conv operator at hidden layer l , and let $I^{(l,\gamma,j)} \subset [N]$ be its receptive field. By the structure of the network it is evident that $I^{(l,\gamma,j)}$ does not depend on γ , so we may write $I^{(l,j)}$ instead. Moreover, assuming pooling windows are uniform across channels (as customary for convolutional networks), and taking into account the fact that they do not overlap, we conclude that $I^{(l,j_1)}$ and $I^{(l,j_2)}$ are necessarily disjoint if $j_1 \neq j_2$. A simple induction over $l = 0 \dots L-1$ then shows that $h_{(l,\gamma,j)}$ may be expressed as $h_{(l,\gamma,j)}(\mathbf{x}_{i_1}, \dots, \mathbf{x}_{i_T}) = \sum_{d_1 \dots d_T=1}^M \mathcal{A}_{d_1 \dots d_T}^{(l,\gamma,j)} \prod_{t=1}^T f_{\theta_{d_t}}(\mathbf{x}_{i_t})$, where $\{i_1, \dots, i_T\}$ stands for the receptive field $I^{(l,j)}$, and $\mathcal{A}^{(l,\gamma,j)}$ is a tensor of order $T = |I^{(l,j)}|$ and dimension M in each mode, with entries given by polynomials in the network's conv weights ($\{\mathbf{a}^{l,\gamma}\}_{l,\gamma}$). Taking the induction one step further (from last hidden layer to network output), we obtain the following expression for functions realized by network outputs:

$$h_y(\mathbf{x}_1, \dots, \mathbf{x}_N) = \sum_{d_1 \dots d_N=1}^M \mathcal{A}_{d_1, \dots, d_N}^y \prod_{i=1}^N f_{\theta_{d_i}}(\mathbf{x}_i) \quad (2)$$

$y \in [Y]$ here is an output node index, and h_y is the function realized by that node. \mathcal{A}^y is a tensor of order N and dimension M in each mode, with entries given by polynomials in the network's conv weights $\{\mathbf{a}^{l,\gamma}\}_{l,\gamma}$ and output weights $\mathbf{a}^{L,y}$. Hereafter, terms such as *function realized by a network* or *coefficient tensor realized by a network*, are to be understood as referring to h_y or \mathcal{A}^y respectively. Next, we present explicit expressions for \mathcal{A}^y under two canonical networks – deep and shallow.

Deep network. Consider a network as in fig. 1(a), with pooling windows set to cover four entries each, resulting in $L = \log_4 N$ hidden layers. The linear weights of such a network are $\{\mathbf{a}^{0,\gamma} \in \mathbb{R}^M\}_{\gamma \in [r_0]}$ for conv operator in hidden layer 0, $\{\mathbf{a}^{l,\gamma} \in \mathbb{R}^{r_{l-1}}\}_{\gamma \in [r_l]}$ for conv operator in hidden layer $l = 1 \dots L-1$, and $\{\mathbf{a}^{L,y} \in \mathbb{R}^{r_{L-1}}\}_{y \in [Y]}$ for dense output operator. They determine the coefficient tensor \mathcal{A}^y (eq. 2) through the following recursive decomposition:

$$\begin{aligned} \underbrace{\phi_\alpha^{1,\gamma}}_{\text{order } 4} &= \sum_{\alpha=1}^{r_0} a_\alpha^{1,\gamma} \cdot \otimes^4 \mathbf{a}^{0,\alpha} \quad , \gamma \in [r_1] \\ &\dots \\ \underbrace{\phi_\alpha^{l,\gamma}}_{\text{order } 4^l} &= \sum_{\alpha=1}^{r_{l-1}} a_\alpha^{l,\gamma} \cdot \otimes^4 \phi^{l-1,\alpha} \quad , l \in \{2 \dots L-1\}, \gamma \in [r_l] \\ &\dots \\ \underbrace{\mathcal{A}^y}_{\text{order } 4^{L=N}} &= \sum_{\alpha=1}^{r_{L-1}} a_\alpha^{L,y} \cdot \otimes^4 \phi^{L-1,\alpha} \end{aligned} \quad (3)$$

$a_\alpha^{l,\gamma}$ and $a_\alpha^{L,y}$ here are scalars representing entry α in the vectors $\mathbf{a}^{l,\gamma}$ and $\mathbf{a}^{L,y}$ respectively, and the symbol \otimes with a superscript stands for a repeated tensor product, e.g. $\otimes^4 \mathbf{a}^{0,\alpha} := \mathbf{a}^{0,\alpha} \otimes \mathbf{a}^{0,\alpha} \otimes \mathbf{a}^{0,\alpha} \otimes \mathbf{a}^{0,\alpha}$. To verify that under pooling windows of size four \mathcal{A}^y is indeed given by eq. 3, simply plug the rows of the decomposition into eq. 2, starting from bottom and continuing upwards. For context, eq. 3 describes what is called a hierarchical tensor decomposition (see chapter 11 in [12]), with underlying tree over modes being a full quad-tree (corresponding to the fact that the network's pooling windows cover four entries each).

Shallow network. The second network we pay special attention to is shallow, comprising a single hidden layer with global pooling – see illustration in fig. 1(b). The linear weights of such a network are $\{\mathbf{a}^{0,\gamma} \in \mathbb{R}^M\}_{\gamma \in [r_0]}$ for hidden conv operator and $\{\mathbf{a}^{1,y} \in \mathbb{R}^{r_0}\}_{y \in [Y]}$ for dense output operator. They determine the coefficient tensor \mathcal{A}^y (eq. 2) as follows:

$$\mathcal{A}^y = \sum_{\gamma=1}^{r_0} a_{\gamma}^{1,y} \cdot \otimes^N \mathbf{a}^{0,\gamma} \quad (4)$$

where $a_{\gamma}^{1,y}$ stands for entry γ of $\mathbf{a}^{1,y}$, and again, the symbol \otimes with a superscript represents a repeated tensor product. The tensor decomposition in eq. 4 is an instance of the classic CP decomposition, also known as rank-1 decomposition (see [16] for a historic survey).

To conclude this section, we relate the background material above, as well as our contribution described in the upcoming sections, to the work of [8]. The latter shows that for arbitrary coefficient tensors \mathcal{A}^y , functions h_y as in eq. 2 form a universal hypotheses space. It is then shown that convolutional arithmetic circuits as in fig. 1(a) realize such functions by applying tensor decompositions to \mathcal{A}^y , with the type of decomposition determined by the structure of a network (number of layers, number of channels in each layer *etc.*). The deep network (fig. 1(a) with size-4 pooling windows and $L = \log_4 N$ hidden layers) and the shallow network (fig. 1(b)) presented hereinabove are two special cases, whose corresponding tensor decompositions are given in eq. 3 and 4 respectively. The central result in [8] relates to inductive bias through the notion of *depth efficiency* – it is shown that in the parameter space of a deep network, all weight settings but a set of measure zero give rise to functions that can only be realized (or approximated) by a shallow network if the latter has exponential size. This result does not relate to the characteristics of instances $X = (\mathbf{x}_1, \dots, \mathbf{x}_N)$, it only treats the ability of shallow networks to replicate functions realized by deep networks.

In this paper we draw a line connecting the inductive bias to the nature of X , by studying the relation between a network’s architecture and its ability to model correlation among patches \mathbf{x}_i . Specifically, in sec. 4 we consider partitions (I, J) of $[N]$ ($I \cup J = [N]$, where \cup stands for disjoint union), and present the notion of separation rank as a measure of the correlation modeled between patches indexed by I and ones indexed by J . In sec. 5.1 the separation rank of a network’s function h_y w.r.t. a partition (I, J) is proven to be equal to the rank of $\llbracket \mathcal{A}^y \rrbracket_{I,J}$ – the matricization w.r.t. (I, J) of the coefficient tensor \mathcal{A}^y . Sec. 5.2 derives lower and upper bounds on this rank for a deep network, showing that it supports exponential separation ranks with polynomial size for certain partitions, whereas for others it is required to be exponentially large. Subsequently, sec. 5.3 establishes an upper bound on $\text{rank} \llbracket \mathcal{A}^y \rrbracket_{I,J}$ for shallow networks, implying that these must be exponentially large in order to model exponential separation rank under any partition, and thus cannot efficiently replicate a deep network’s correlations. Our analysis is concluded in sec. 6, which discusses the pooling geometry of a deep network as a means for controlling the inductive bias by determining a correspondence between partitions (I, J) and spatial partitions of the input.

4 Separation rank

In this section we define the concept of separation rank for functions realized by convolutional arithmetic circuits (sec. 3), *i.e.* functions that take as input $X = (\mathbf{x}_1, \dots, \mathbf{x}_N) \in (\mathbb{R}^s)^N$. The separation rank serves as a measure of the correlations such functions induce between different sets of input patches, *i.e.* different subsets of the variable set $\{\mathbf{x}_1, \dots, \mathbf{x}_N\}$.

Let (I, J) be a partition of input indexes, *i.e.* I and J are disjoint subsets of $[N]$ whose union gives $[N]$. We may write $I = \{i_1, \dots, i_{|I|}\}$ where $i_1 < \dots < i_{|I|}$, and similarly $J = \{j_1, \dots, j_{|J|}\}$ where $j_1 < \dots < j_{|J|}$. For a function $h : (\mathbb{R}^s)^N \rightarrow \mathbb{R}$, the *separation rank w.r.t. the partition (I, J)* is defined as follows:²

$$\text{sep}(h; I, J) := \min \left\{ R \in \mathbb{N} \cup \{0\} : \exists g_1 \dots g_R : (\mathbb{R}^s)^{|I|} \rightarrow \mathbb{R}, g'_1 \dots g'_R : (\mathbb{R}^s)^{|J|} \rightarrow \mathbb{R} \text{ s.t.} \right. \quad (5)$$

$$\left. h(\mathbf{x}_1, \dots, \mathbf{x}_N) = \sum_{\nu=1}^R g_{\nu}(\mathbf{x}_{i_1}, \dots, \mathbf{x}_{i_{|I|}}) g'_{\nu}(\mathbf{x}_{j_1}, \dots, \mathbf{x}_{j_{|J|}}) \right\}$$

In words, it is the minimal number of summands that together give h , where each summand is equal to a product of two functions – one that intakes only patches indexed by I , and another that

² If $I = \emptyset$ or $J = \emptyset$ then by definition $\text{sep}(h; I, J) = 1$ (unless $h \equiv 0$, in which case $\text{sep}(h; I, J) = 0$).

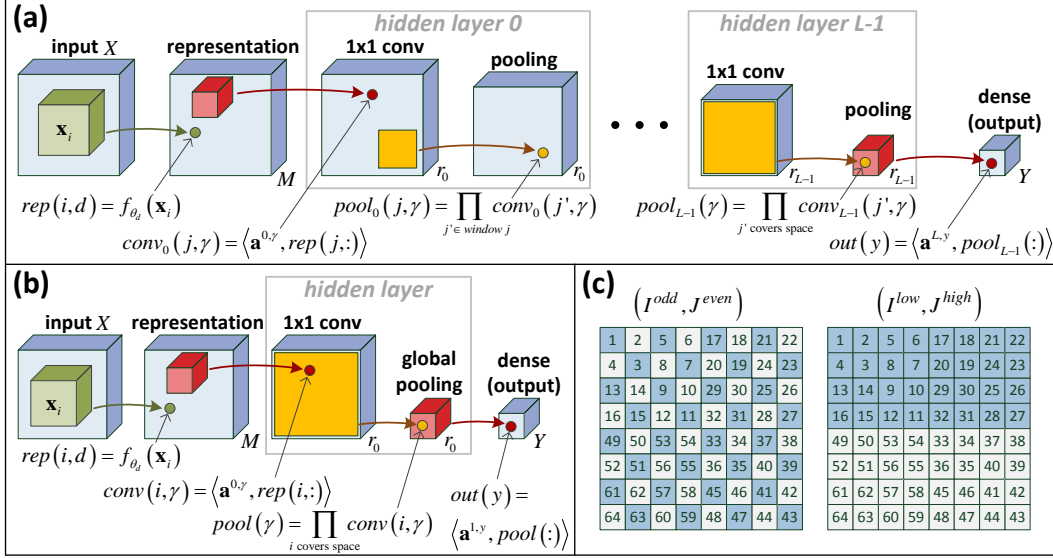


Figure 1: Best viewed in color. **(a)** Convolutional arithmetic circuit architecture analyzed in this paper (see description in sec. 3). **(b)** Shallow network with global pooling in its single hidden layer. **(c)** Illustration of input patch ordering for deep network with 2×2 pooling windows, along with patterns induced by the partitions (I^{odd}, J^{even}) and (I^{low}, J^{high}) (eq. 8 and 9 respectively).

intakes only patches indexed by J . One may wonder if it is at all possible to express h through such summands, *i.e.* if the separation rank of h is finite. From the theory of tensor products between L^2 spaces (see [12] for a comprehensive coverage), we know that any $h \in L^2((\mathbb{R}^s)^N)$, *i.e.* any h that is measurable and square integrable, may be approximated arbitrarily well by summations of the form $\sum_{\nu=1}^R g_{\nu}(x_{i_1}, \dots, x_{i_{|I|}}) g'_{\nu}(x_{j_1}, \dots, x_{j_{|J|}})$. Exact realization however is only guaranteed at the limit $R \rightarrow \infty$, thus in general the separation rank of h need not be finite. Nonetheless, as we show in sec. 5, for the class of functions we are interested in, namely functions realizable by convolutional arithmetic circuits, separation ranks are always finite.

The concept of separation rank was introduced in [2] for numerical treatment of high-dimensional functions. Since then, it has been employed for various applications, including quantum chemistry ([13]), particle engineering ([11]), machine learning ([3]), and more. The separation rank measures how separable function variables are, or conversely, how correlated they are in determining function values. When separation rank equals 1, function variables are completely separable, meaning they are completely uncorrelated in determining function values. On the other hand, high separation rank indicates that function variables are difficult to separate, *i.e.* the function induces strong correlation between them. In our context, the separation rank of a function $h : (\mathbb{R}^s)^N \rightarrow \mathbb{R}$ w.r.t. the partition (I, J) of $[N]$ (eq. 5), measures the strength of the modeled correlation between two sets of input patches – those indexed by I ($x_{i_1} \dots x_{i_{|I|}}$), and those indexed by J ($x_{j_1} \dots x_{j_{|J|}}$).

5 Correlation analysis

In this section we analyze convolutional arithmetic circuits (sec. 3) in terms of the correlations they model between sides of different input partitions, *i.e.* in terms of the separation ranks (sec. 4) they support under different partitions (I, J) of $[N]$. We begin in sec. 5.1, establishing a correspondence between separation ranks and coefficient tensor matricization ranks. This correspondence is then used in sec. 5.2 and 5.3 to analyze the deep and shallow networks (respectively) presented in sec. 3. We note that we focus on these particular networks merely for simplicity of presentation – the analysis can easily be adapted to account for alternative networks with different depths and pooling schemes.

5.1 From separation rank to matricization rank

Let h_y be a function realized by a convolutional arithmetic circuit, with corresponding coefficient tensor \mathcal{A}^y (eq. 2). Denote by (I, J) an arbitrary partition of $[N]$, *i.e.* $I \cup J = [N]$. We are interested

in studying $\text{sep}(h_y; I, J)$ – the separation rank of h_y w.r.t. (I, J) (eq. 5). As claim 1 below states, assuming representation functions $\{f_{\theta_d}\}_{d \in [M]}$ are linearly independent (there is no reason to choose them otherwise³), this separation rank is equal to the rank of $\llbracket \mathcal{A}^y \rrbracket_{I,J}$ – the matricization of the coefficient tensor \mathcal{A}^y w.r.t. the partition (I, J) . Our problem thus translates to studying ranks of matricized coefficient tensors.

Claim 1. *Let h_y be a function realized by a convolutional arithmetic circuit (fig. 1(a)), with corresponding coefficient tensor \mathcal{A}^y (eq. 2). Assume that the network’s representation functions (f_{θ_d}) are linearly independent, and consider an arbitrary partition (I, J) of $[N]$. Then $\text{sep}(h_y; I, J) = \text{rank} \llbracket \mathcal{A}^y \rrbracket_{I,J}$.*

Proof. See app. A.1. □

As the linear weights of a network vary, so do the coefficient tensors it gives rise to (\mathcal{A}^y). Accordingly, for a particular partition (I, J) , a network does not correspond to a single value of $\text{rank} \llbracket \mathcal{A}^y \rrbracket_{I,J}$, but rather supports a range of values. We analyze this range by quantifying its maximum, which reflects the strongest correlation that the network can model between the input patches indexed by I and those indexed by J . One may wonder if the maximal value of $\text{rank} \llbracket \mathcal{A}^y \rrbracket_{I,J}$ is the appropriate statistic to measure, as a-priori, it may be that $\text{rank} \llbracket \mathcal{A}^y \rrbracket_{I,J}$ is maximal for very few of the network’s weight settings, and much lower for all the rest. Apparently, as claim 2 below shows, this is not the case, and in fact $\text{rank} \llbracket \mathcal{A}^y \rrbracket_{I,J}$ is maximal under almost all of the network’s weight settings.

Claim 2. *Consider a convolutional arithmetic circuit (fig. 1(a)) with corresponding coefficient tensor \mathcal{A}^y (eq. 2). \mathcal{A}^y depends on the network’s linear weights – $\{\mathbf{a}^{l,\gamma}\}_{l,\gamma}$ and $\mathbf{a}^{L,y}$, thus for a given partition (I, J) of $[N]$, $\text{rank} \llbracket \mathcal{A}^y \rrbracket_{I,J}$ is a function of these weights. This function obtains its maximum almost everywhere (w.r.t. Lebesgue measure).*

Proof. See app. A.2. □

5.2 Deep network

In this subsection we study correlations modeled by the deep network presented in sec. 3 (fig. 1(a) with size-4 pooling windows and $L = \log_4 N$ hidden layers). In accordance with sec. 5.1, we do so by characterizing the maximal ranks of coefficient tensor matricizations under different partitions.

Recall from eq. 3 the hierarchical decomposition expressing a coefficient tensor \mathcal{A}^y realized by the deep network. We are interested in matricizations of this tensor under different partitions of $[N]$. Let (I, J) be an arbitrary partition, i.e. $I \cup J = [N]$. Matricizing the last row of eq. 3 w.r.t. (I, J) , while applying the relation in eq. 1, gives:

$$\begin{aligned} \llbracket \mathcal{A}^y \rrbracket_{I,J} &= \sum_{\alpha=1}^{r^{L-1}} a_{\alpha}^{L,y} \cdot \llbracket \phi^{L-1,\alpha} \otimes \phi^{L-1,\alpha} \otimes \phi^{L-1,\alpha} \otimes \phi^{L-1,\alpha} \rrbracket_{I,J} \\ &= \sum_{\alpha=1}^{r^{L-1}} a_{\alpha}^{L,y} \cdot \llbracket \phi^{L-1,\alpha} \otimes \phi^{L-1,\alpha} \rrbracket_{I \cap [2 \cdot 4^{L-1}], J \cap [2 \cdot 4^{L-1}]} \\ &\quad \odot \llbracket \phi^{L-1,\alpha} \otimes \phi^{L-1,\alpha} \rrbracket_{(I - 2 \cdot 4^{L-1}) \cap [2 \cdot 4^{L-1}], (J - 2 \cdot 4^{L-1}) \cap [2 \cdot 4^{L-1}]} \end{aligned}$$

Applying eq. 1 again, this time to matricizations of the tensor $\phi^{L-1,\alpha} \otimes \phi^{L-1,\alpha}$, we obtain:

$$\begin{aligned} \llbracket \mathcal{A}^y \rrbracket_{I,J} &= \sum_{\alpha=1}^{r^{L-1}} a_{\alpha}^{L,y} \cdot \llbracket \phi^{L-1,\alpha} \rrbracket_{I \cap [4^{L-1}], J \cap [4^{L-1}]} \\ &\quad \odot \llbracket \phi^{L-1,\alpha} \rrbracket_{(I - 4^{L-1}) \cap [4^{L-1}], (J - 4^{L-1}) \cap [4^{L-1}]} \\ &\quad \odot \llbracket \phi^{L-1,\alpha} \rrbracket_{(I - 2 \cdot 4^{L-1}) \cap [4^{L-1}], (J - 2 \cdot 4^{L-1}) \cap [4^{L-1}]} \\ &\quad \odot \llbracket \phi^{L-1,\alpha} \rrbracket_{(I - 3 \cdot 4^{L-1}) \cap [4^{L-1}], (J - 3 \cdot 4^{L-1}) \cap [4^{L-1}]} \end{aligned}$$

For every $k \in [4]$ define $I_{L-1,k} := (I - (k-1) \cdot 4^{L-1}) \cap [4^{L-1}]$ and $J_{L-1,k} := (J - (k-1) \cdot 4^{L-1}) \cap [4^{L-1}]$. In words, $(I_{L-1,k}, J_{L-1,k})$ represents the partition induced by (I, J) on the k ’th

³ The case of linearly dependent representation functions is degenerate, equivalent to reducing the number of channels in the representation layer (M).

quadrant of $[N]$, *i.e.* on the k 'th size- 4^{L-1} group of input patches. We now have the following matricized version of the last level in eq. 3:

$$\llbracket \mathcal{A}^y \rrbracket_{I,J} = \sum_{\alpha=1}^{r_{L-1}} a_{\alpha}^{L,y} \cdot \bigodot_{t=1}^4 \llbracket \phi^{L-1,\alpha} \rrbracket_{I_{L-1,t}, J_{L-1,t}}$$

where the symbol \odot with a running index stands for an iterative Kronecker product. To derive analogous matricized versions for the upper levels of eq. 3, we define for $l \in \{0 \dots L-1\}$, $k \in [N/4^l]$:

$$I_{l,k} := (I - (k-1) \cdot 4^l) \cap [4^l] \quad J_{l,k} := (J - (k-1) \cdot 4^l) \cap [4^l] \quad (6)$$

That is to say, $(I_{l,k}, J_{l,k})$ represents the partition induced by (I, J) on the set of indexes $\{(k-1) \cdot 4^l + 1, \dots, k \cdot 4^l\}$, *i.e.* on the k 'th size- 4^l group of input patches. With this notation in hand, traversing upwards through the levels of eq. 3, with repeated application of the relation in eq. 1, one arrives at the following matrix decomposition for $\llbracket \mathcal{A}^y \rrbracket_{I,J}$:

$$\begin{aligned} \underbrace{\llbracket \phi^{1,\gamma} \rrbracket_{I_{1,k}, J_{1,k}}}_{M^{|I_{1,k}|} \text{-by-} M^{|J_{1,k}|}} &= \sum_{\alpha=1}^{r_0} a_{\alpha}^{1,\gamma} \cdot \bigodot_{t=1}^4 \llbracket \mathbf{a}^{0,\alpha} \rrbracket_{I_{0,4(k-1)+t}, J_{0,4(k-1)+t}} \quad , \gamma \in [r_1] \\ &\dots \\ \underbrace{\llbracket \phi^{l,\gamma} \rrbracket_{I_{l,k}, J_{l,k}}}_{M^{|I_{l,k}|} \text{-by-} M^{|J_{l,k}|}} &= \sum_{\alpha=1}^{r_{l-1}} a_{\alpha}^{l,\gamma} \cdot \bigodot_{t=1}^4 \llbracket \phi^{l-1,\alpha} \rrbracket_{I_{l-1,4(k-1)+t}, J_{l-1,4(k-1)+t}} \quad , l \in \{2 \dots L-1\}, \gamma \in [r_l] \\ &\dots \\ \underbrace{\llbracket \mathcal{A}^y \rrbracket_{I,J}}_{M^{|I|} \text{-by-} M^{|J|}} &= \sum_{\alpha=1}^{r_{L-1}} a_{\alpha}^{L,y} \cdot \bigodot_{t=1}^4 \llbracket \phi^{L-1,\alpha} \rrbracket_{I_{L-1,t}, J_{L-1,t}} \end{aligned} \quad (7)$$

Eq. 7 expresses $\llbracket \mathcal{A}^y \rrbracket_{I,J}$ – the matricization w.r.t. the partition (I, J) of a coefficient tensor \mathcal{A}^y realized by the deep network, in terms of the network's conv weights $\{\mathbf{a}^{l,\gamma}\}_{l,\gamma}$ and output weights $\mathbf{a}^{L,y}$. As discussed in sec. 5.1, our interest lies in the maximal rank that this matricization can take. Theorem 1 below provides lower and upper bounds on this maximal rank, by making use of eq. 7, and of the rank-multiplicative property of the Kronecker product ($\text{rank}(A \odot B) = \text{rank}(A) \cdot \text{rank}(B)$).

Theorem 1. *Let (I, J) be a partition of $[N]$, and $\llbracket \mathcal{A}^y \rrbracket_{I,J}$ be the matricization w.r.t. (I, J) of a coefficient tensor \mathcal{A}^y (eq. 2) realized by the deep network (fig. 1(a) with size-4 pooling windows). For every $l \in \{0 \dots L-1\}$ and $k \in [N/4^l]$, define $I_{l,k}$ and $J_{l,k}$ as in eq. 6. Then, the maximal rank that $\llbracket \mathcal{A}^y \rrbracket_{I,J}$ can take (when network weights vary) is:*

- No smaller than $\min\{r_0, M\}^S$, where $S := |\{k \in [N/4] : I_{1,k} \neq \emptyset \wedge J_{1,k} \neq \emptyset\}|$.
- No greater than $\min\{M^{\min\{|I|, |J|\}}, r_{L-1} \prod_{t=1}^4 c^{L-1,t}\}$, where $c^{0,k} := 1$ for $k \in [N]$, and $c^{l,k} := \min\{M^{\min\{|I_{l,k}|, |J_{l,k}|\}}, r_{l-1} \prod_{t=1}^4 c^{l-1,4(k-1)+t}\}$ for $l \in [L-1]$, $k \in [N/4^l]$.

Proof. See app. A.3. □

The lower bound in theorem 1 is exponential in S , the latter defined to be the number of size-4 patch groups that are split by the partition (I, J) , *i.e.* whose indexes are divided between I and J . Partitions that split many of the size-4 patch groups will thus lead to a large lower bound. For example, consider the partition $(I^{\text{odd}}, J^{\text{even}})$ defined as follows:

$$I^{\text{odd}} = \{1, 3, \dots, N-1\} \quad J^{\text{even}} = \{2, 4, \dots, N\} \quad (8)$$

This partition splits all size-4 patch groups ($S = N/4$), leading to a lower bound that is exponential in the number of patches (N).

The upper bound in theorem 1 is expressed via constants $c^{l,k}$, defined recursively over levels $l = 0 \dots L-1$, with k ranging over $1 \dots N/4^l$ for each level l . What prevents $c^{l,k}$ from growing double-exponentially fast (w.r.t. l) is the minimization with $M^{\min\{|I_{l,k}|, |J_{l,k}|\}}$. Specifically, if $\min\{|I_{l,k}|, |J_{l,k}|\}$ is small, *i.e.* if the partition induced by (I, J) on the k 'th size- 4^l group of patches is unbalanced (most of the patches belong to one side of the partition, and only a few belong to the

other), $c^{l,k}$ will be of reasonable size. The higher this takes place in the hierarchy (*i.e.* the larger l is), the lower our eventual upper bound will be. In other words, if partitions induced by (I, J) on size- 4^l patch groups are unbalanced for large values of l , the upper bound in theorem 1 will be small. For example, consider the partition (I^{low}, J^{high}) defined by:

$$I^{low} = \{1, \dots, N/2\} \quad J^{high} = \{N/2 + 1, \dots, N\} \quad (9)$$

Under (I^{low}, J^{high}) , all partitions induced on size- 4^{L-1} patch groups (quadrants of $[N]$) are completely one-sided ($\min\{|I_{L-1,k}|, |J_{L-1,k}|\} = 0$ for all $k \in [4]$), resulting in the upper bound being no greater than r_{L-1} – linear in network size.

To summarize this discussion, theorem 1 states that with the deep network, the maximal rank of a coefficient tensor matricization w.r.t. (I, J) , highly depends on the nature of the partition (I, J) – it will be exponentially large for partitions such as (I^{odd}, J^{even}) , that split many size-4 patch groups, while being only polynomial (or linear) for partitions like (I^{low}, J^{high}) , under which size- 4^l patch groups are unevenly divided for large values of l . Since the rank of a coefficient tensor matricization w.r.t. (I, J) corresponds to the strength of correlation modeled between input patches indexed by I and those indexed by J (sec. 5.1), we conclude that the ability of a polynomially sized deep network to model correlation between sets of input patches highly depends on the nature of these sets.

5.3 Shallow network

We now turn to study correlations modeled by the shallow network presented in sec. 3 (fig. 1(b)). In line with sec. 5.1, this is achieved by characterizing the maximal ranks of coefficient tensor matricizations under different partitions.

Recall from eq. 4 the CP decomposition expressing a coefficient tensor \mathcal{A}^y realized by the shallow network. For an arbitrary partition (I, J) of $[N]$, *i.e.* $I \cup J = [N]$, matricizing this decomposition with repeated application of the relation in eq. 1, gives the following expression for $\llbracket \mathcal{A}^y \rrbracket_{I,J}$ – the matricization w.r.t. (I, J) of a coefficient tensor realized by the shallow network:

$$\llbracket \mathcal{A}^y \rrbracket_{I,J} = \sum_{\gamma=1}^{r_0} a_{\gamma}^{1,y} \cdot \left(\odot^{|I|} \mathbf{a}^{0,\gamma} \right) \left(\odot^{|J|} \mathbf{a}^{0,\gamma} \right)^{\top} \quad (10)$$

$\odot^{|I|} \mathbf{a}^{0,\gamma}$ and $\odot^{|J|} \mathbf{a}^{0,\gamma}$ here are column vectors of dimensions $M^{|I|}$ and $M^{|J|}$ respectively, standing for the Kronecker products of $\mathbf{a}^{0,\gamma} \in \mathbb{R}^M$ with itself $|I|$ and $|J|$ times (respectively). Eq. 10 immediately leads to two observations regarding the ranks that may be taken by $\llbracket \mathcal{A}^y \rrbracket_{I,J}$. First, they depend on the partition (I, J) only through its division size, *i.e.* through $|I|$ and $|J|$. Second, they are no greater than $\min\{M^{\min\{|I|, |J|\}}, r_0\}$, meaning that the maximal rank is linear (or less) in network size. In light of sec. 5.1 and 5.2, these findings imply that in contrast to the deep network, which with polynomial size supports exponential separation ranks under favored partitions, the shallow network treats all partitions (of a given division size) equally, and can only give rise to an exponential separation rank if its size is exponential.

Suppose now that we would like to use the shallow network to replicate a function realized by a polynomially sized deep network. So long as the deep network’s function realizes an exponential separation rank under at least one of the favored partitions (*e.g.* (I^{odd}, J^{even}) – eq. 8), the shallow network would have to be exponentially large in order to replicate it⁴, *i.e.* depth efficiency takes place. Since all but a negligible set of the functions realizable by the deep network give rise to maximal separation ranks (claim 2), we obtain the complete depth efficiency result of [8]. However, unlike [8], which did not provide any explanation for the usefulness of functions brought forth by depth, we obtain an insight into their utility – they are able to efficiently model strong correlation between favored partitions of the input.

⁴ Our definition of the shallow network includes weight sharing in its hidden conv operator. By eq. 4, this implies that the network is not universal (may only realize symmetric coefficient tensors), and thus might not be able to replicate the deep network’s function, no matter how large we allow it to be. However, even if we consider the more powerful, universal variant of the shallow network which is not constrained by weight sharing, the exact same results would hold. In particular, the separation ranks of the network would still be linear in its size, and we would still have (complete) depth efficiency.

6 Inductive bias through pooling geometry

The deep network presented in sec. 3, whose correlations we analyzed in sec. 5.2, was defined as having size-4 pooling windows, *i.e.* pooling windows covering four entries each. We have yet to specify the shapes of these windows, or equivalently, the spatial (two-dimensional) locations of nodes grouped together in the process of pooling. In compliance with standard convolutional network design, we now assume that the network’s (size-4) pooling windows are contiguous square blocks, *i.e.* have shape 2×2 . Under this configuration, the network’s functional description (eq. 2 with \mathcal{A}^y given by eq. 3) induces a spatial ordering of input patches⁵, which may be described by the following recursive process:

- Set the index of the top-left patch to 1.
- For $l = 1, \dots, L = \log_4 N$: Replicate the already-assigned top-left 2^{l-1} -by- 2^{l-1} block of indexes, and place copies on its right, bottom-right and bottom. Then, add a 4^{l-1} offset to all indexes in the right copy, a $2 \cdot 4^{l-1}$ offset to all indexes in the bottom-right copy, and a $3 \cdot 4^{l-1}$ offset to all indexes in the bottom copy.

With this spatial ordering (illustrated in fig. 1(c)), partitions (I, J) of $[N]$ convey a spatial pattern. For example, the partition (I^{odd}, J^{even}) (eq. 8) corresponds to the pattern illustrated on the left of fig. 1(c), whereas (I^{low}, J^{high}) (eq. 9) corresponds to the pattern illustrated on the right. Our analysis (sec. 5.2) shows that the deep network is able to model strong correlation under (I^{odd}, J^{even}) , while being inefficient for modeling correlation under (I^{low}, J^{high}) . More generally, partitions for which S , defined in theorem 1, is high, convey patterns that split many 2×2 patch blocks, *i.e.* are highly entangled. These partitions enjoy the possibility of strong correlation. On the other hand, partitions for which $\min\{|I_{l,k}|, |J_{l,k}|\}$ is small for large values of l (see eq. 6 for definition of $I_{l,k}$ and $J_{l,k}$) convey patterns that divide large $2^l \times 2^l$ patch blocks unevenly, *i.e.* separate the input to distinct contiguous regions. These partitions, as we have seen, suffer from limited low correlations.

We conclude that with 2×2 pooling, the deep network is able to model strong correlation between input regions that are highly entangled, at the expense of being inefficient for modeling correlation between input regions that are far apart. Had we selected a different pooling regime, the preference of input partition patterns in terms of modeled correlation would change. For example, if nodes grouped together by a pooling window were matching elements in the four quadrants of a feature map (in which case pooling windows are highly noncontiguous), the correlations corresponding to the two patterns illustrated in fig. 1(c) would swap – the entangled pattern on the left would now suffer from limited low correlation, whereas the coarse one on the right would enjoy the possibility of strong correlation. The choice of pooling shapes thus serves as a means for controlling the inductive bias in terms of correlations modeled under different input partitions. Square contiguous windows, as commonly employed in practice, lead to a preference of interleaved partitions over coarse ones, in compliance with our intuition regarding the statistics of natural images (nearby pixels are more correlated than distant ones).

7 Discussion

Through the notion of separation rank, we studied the relation between the architecture of a convolutional arithmetic circuit, and its ability to model correlations among input regions. For a given input partition, the separation rank quantifies how far a function is from being separable, *i.e.* from being equal to a product of terms, each depending on input regions from only one side of the partition.

Our analysis shows that a polynomially sized deep network supports exponentially high separation ranks for certain input partitions, while being limited to polynomial or linear (in network size) separation ranks for others. The network’s pooling window shapes effectively determine which input

⁵ The network’s functional description assumes a one-dimensional full quad-tree grouping of input patch indexes. That is to say, it assumes that in the first pooling operation (hidden layer 0), the nodes corresponding to patches $\mathbf{x}_1, \mathbf{x}_2, \mathbf{x}_3, \mathbf{x}_4$ are pooled into one group, those corresponding to $\mathbf{x}_5, \mathbf{x}_6, \mathbf{x}_7, \mathbf{x}_8$ are pooled into another, and so forth. Similar assumptions hold for the deeper layers. For example, in the second pooling operation (hidden layer 1), the node with receptive field $\{1, 2, 3, 4\}$, *i.e.* the one corresponding to the quadruple of patches $\{\mathbf{x}_1, \mathbf{x}_2, \mathbf{x}_3, \mathbf{x}_4\}$, is assumed to be pooled together with the nodes whose receptive fields are $\{5, 6, 7, 8\}$, $\{9, 10, 11, 12\}$ and $\{13, 14, 15, 16\}$.

partitions are favored in terms of separation rank, *i.e.* which partitions enjoy exponentially high separation ranks with polynomially sized networks, and which require networks to be exponentially large. Pooling geometry thus serves as a means for controlling the inductive bias of deep networks. The particular pooling scheme commonly employed in practice – square contiguous windows, favors interleaved partitions over ones that divide the input to distinct areas, and thus orients the inductive bias towards the statistics of natural images (nearby pixels more correlated than distant ones).

As opposed to deep networks, shallow networks support only linear (in network size) separation ranks. Therefore, in order to replicate a function realized by a deep network (exponential separation rank), a shallow network must be exponentially large. By this we derive the depth efficiency result of [8], but in addition, provide an insight into the benefit of functions brought forth by depth – they are able to efficiently model strong correlation under favored partitions of the input.

Finally, the selection of correlation-wise favored input partitions through a deep network’s pooling geometry, enables tailoring the inductive bias to data that does not necessarily comply with the statistics of natural images. Suppose for example that we would like to detect symmetry between the left and right halves of a CT scan. With the standard arrangement of pooling windows (contiguous square blocks), the left-vs.-right halving partition is unfavored, and thus a very large network would be required in order to model the desired correlation. By modifying the network’s pooling regime (to incorporate noncontiguous windows), we may turn this partition favorable, and thus enable use of a much smaller network.

Acknowledgments

This work is partly funded by Intel grant ICRI-CI no. 9-2012-6133 and by ISF Center grant 1790/12. Nadav Cohen is supported by a Google Fellowship in Machine Learning.

References

- [1] Richard Bellman, Richard Ernest Bellman, Richard Ernest Bellman, and Richard Ernest Bellman. *Introduction to matrix analysis*, volume 960. SIAM, 1970.
- [2] Gregory Beylkin and Martin J Mohlenkamp. Numerical operator calculus in higher dimensions. *Proceedings of the National Academy of Sciences*, 99(16):10246–10251, 2002.
- [3] Gregory Beylkin, Jochen Garcke, and Martin J Mohlenkamp. Multivariate regression and machine learning with sums of separable functions. *SIAM Journal on Scientific Computing*, 31(3):1840–1857, 2009.
- [4] Richard Caron and Tim Traynor. The zero set of a polynomial. *WSMR Report 05-02*, 2005.
- [5] Nadav Cohen and Amnon Shashua. Simnets: A generalization of convolutional networks. *Advances in Neural Information Processing Systems (NIPS), Deep Learning Workshop*, 2014.
- [6] Nadav Cohen and Amnon Shashua. Convolutional rectifier networks as generalized tensor decompositions. *International Conference on Machine Learning (ICML)*, 2016.
- [7] Nadav Cohen, Or Sharir, and Amnon Shashua. Deep simnets. *IEEE Conference on Computer Vision and Pattern Recognition (CVPR)*, 2016.
- [8] Nadav Cohen, Or Sharir, and Amnon Shashua. On the expressive power of deep learning: A tensor analysis. *Conference On Learning Theory (COLT)*, 2016.
- [9] Olivier Delalleau and Yoshua Bengio. Shallow vs. deep sum-product networks. In *Advances in Neural Information Processing Systems*, pages 666–674, 2011.
- [10] Ronen Eldan and Ohad Shamir. The power of depth for feedforward neural networks. *arXiv preprint arXiv:1512.03965*, 2015.
- [11] Wolfgang Hackbusch. On the efficient evaluation of coalescence integrals in population balance models. *Computing*, 78(2):145–159, 2006.
- [12] Wolfgang Hackbusch. *Tensor Spaces and Numerical Tensor Calculus*, volume 42 of *Springer Series in Computational Mathematics*. Springer Science & Business Media, Berlin, Heidelberg, February 2012.
- [13] Robert J Harrison, George I Fann, Takeshi Yanai, and Gregory Beylkin. Multiresolution quantum chemistry in multiwavelet bases. In *Computational Science-ICCS 2003*, pages 103–110. Springer, 2003.

- [14] Kaiming He, Xiangyu Zhang, Shaoqing Ren, and Jian Sun. Deep residual learning for image recognition. *arXiv preprint arXiv:1512.03385*, 2015.
- [15] Frank Jones. *Lebesgue integration on Euclidean space*. Jones & Bartlett Learning, 2001.
- [16] Tamara G Kolda and Brett W Bader. Tensor Decompositions and Applications. *SIAM Review* (), 51(3): 455–500, 2009.
- [17] Alex Krizhevsky, Ilya Sutskever, and Geoffrey E Hinton. ImageNet Classification with Deep Convolutional Neural Networks. *Advances in Neural Information Processing Systems*, pages 1106–1114, 2012.
- [18] Yann LeCun and Yoshua Bengio. Convolutional networks for images, speech, and time series. *The handbook of brain theory and neural networks*, 3361(10), 1995.
- [19] Yann LeCun, Yoshua Bengio, and Geoffrey Hinton. Deep learning. *Nature*, 521(7553):436–444, May 2015.
- [20] Hrushikesh Mhaskar, Qianli Liao, and Tomaso Poggio. Learning real and boolean functions: When is deep better than shallow. *arXiv preprint arXiv:1603.00988*, 2016.
- [21] Guido F Montufar, Razvan Pascanu, Kyunghyun Cho, and Yoshua Bengio. On the number of linear regions of deep neural networks. In *Advances in Neural Information Processing Systems*, pages 2924–2932, 2014.
- [22] Vinod Nair and Geoffrey E Hinton. Rectified linear units improve restricted boltzmann machines. In *Proceedings of the 27th International Conference on Machine Learning (ICML-10)*, pages 807–814, 2010.
- [23] Razvan Pascanu, Guido Montufar, and Yoshua Bengio. On the number of inference regions of deep feed forward networks with piece-wise linear activations. *arXiv preprint arXiv*, 1312, 2013.
- [24] Tomaso Poggio, Fabio Anselmi, and Lorenzo Rosasco. I-theory on depth vs width: hierarchical function composition. Technical report, Center for Brains, Minds and Machines (CBMM), 2015.
- [25] Walter Rudin. Functional analysis. international series in pure and applied mathematics, 1991.
- [26] Karen Simonyan and Andrew Zisserman. Very deep convolutional networks for large-scale image recognition. *arXiv preprint arXiv:1409.1556*, 2014.
- [27] Christian Szegedy, Wei Liu, Yangqing Jia, Pierre Sermanet, Scott Reed, Dragomir Anguelov, Dumitru Erhan, Vincent Vanhoucke, and Andrew Rabinovich. Going Deeper with Convolutions. *CVPR*, 2015.
- [28] Matus Telgarsky. Representation benefits of deep feedforward networks. *arXiv preprint arXiv:1509.08101*, 2015.

A Deferred proofs

A.1 Proof of claim 1

We prove the equality in two steps, first showing that $\text{sep}(h_y; I, J) \leq \text{rank}[\mathcal{A}^y]_{I,J}$, and then establishing the converse. The first part of the proof is elementary, and does not make use of the representation functions' (f_{θ_d}) linear independence. The second part does rely on this assumption, and employs slightly more advanced mathematical machinery. Throughout the proof, we assume without loss of generality that the partition (I, J) of $[N]$ is such that I takes on smaller values, while J takes on larger ones. That is to say, we assume that $I = \{1, \dots, |I|\}$ and $J = \{|I| + 1, \dots, N\}$.⁶

To prove that $\text{sep}(h_y; I, J) \leq \text{rank}[\mathcal{A}^y]_{I,J}$, denote by R the rank of $[\mathcal{A}^y]_{I,J}$. The latter is an $M^{|I|}$ -by- $M^{|J|}$ matrix, thus there exist vectors $\mathbf{u}_1 \dots \mathbf{u}_R \in \mathbb{R}^{M^{|I|}}$ and $\mathbf{v}_1 \dots \mathbf{v}_R \in \mathbb{R}^{M^{|J|}}$ such that $[\mathcal{A}^y]_{I,J} = \sum_{\nu=1}^R \mathbf{u}_\nu \mathbf{v}_\nu^\top$. For every $\nu \in [R]$, let \mathcal{B}^ν be the tensor of order $|I|$ and dimension M in each mode whose arrangement as a column vector gives \mathbf{u}_ν , i.e. whose matricization w.r.t. the partition $([|I|], \emptyset)$ is equal to \mathbf{u}_ν . Similarly, let \mathcal{C}^ν , $\nu \in [R]$, be the tensor of order $|J| = N - |I|$ and dimension M in each mode whose matricization w.r.t. the partition $(\emptyset, [|J|])$ (arrangement as a row vector) is equal to \mathbf{v}_ν^\top . It holds that:

$$\begin{aligned} [\mathcal{A}^y]_{I,J} &= \sum_{\nu=1}^R \mathbf{u}_\nu \mathbf{v}_\nu^\top \\ &= \sum_{\nu=1}^R [\mathcal{B}^\nu]_{[|I|], \emptyset} \odot [\mathcal{C}^\nu]_{\emptyset, [|J|]} \\ &= \sum_{\nu=1}^R [\mathcal{B}^\nu]_{I \cap [|I|], J \cap [|I|]} \odot [\mathcal{C}^\nu]_{(I - |I|) \cap [|J|], (J - |I|) \cap [|J|]} \\ &= \sum_{\nu=1}^R [\mathcal{B}^\nu \otimes \mathcal{C}^\nu]_{I,J} \\ &= \left[\sum_{\nu=1}^R \mathcal{B}^\nu \otimes \mathcal{C}^\nu \right]_{I,J} \end{aligned}$$

where the third equality relies on the assumption $I = \{1, \dots, |I|\}$, $J = \{|I| + 1, \dots, N\}$, the fourth equality makes use of the relation in eq. 1, and the last equality is based on the linearity of the matricization operator. Since matricizations are merely rearrangements of tensors, the fact that $[\mathcal{A}^y]_{I,J} = [\sum_{\nu=1}^R \mathcal{B}^\nu \otimes \mathcal{C}^\nu]_{I,J}$ implies $\mathcal{A}^y = \sum_{\nu=1}^R \mathcal{B}^\nu \otimes \mathcal{C}^\nu$, or equivalently, $\mathcal{A}_{d_1 \dots d_N}^y = \sum_{\nu=1}^R \mathcal{B}_{d_1 \dots d_{|I|}}^\nu \cdot \mathcal{C}_{d_{|I|+1} \dots d_N}^\nu$ for every $d_1 \dots d_N \in [M]$. Plugging the latter into eq. 2 gives:

$$\begin{aligned} h_y(\mathbf{x}_1, \dots, \mathbf{x}_N) &= \sum_{d_1 \dots d_N=1}^M \mathcal{A}_{d_1 \dots d_N}^y \prod_{i=1}^N f_{\theta_{d_i}}(\mathbf{x}_i) \\ &= \sum_{d_1 \dots d_N=1}^M \sum_{\nu=1}^R \mathcal{B}_{d_1 \dots d_{|I|}}^\nu \cdot \mathcal{C}_{d_{|I|+1} \dots d_N}^\nu \prod_{i=1}^N f_{\theta_{d_i}}(\mathbf{x}_i) \\ &= \sum_{\nu=1}^R \left(\sum_{d_1 \dots d_{|I|}=1}^M \mathcal{B}_{d_1 \dots d_{|I|}}^\nu \prod_{i=1}^{|I|} f_{\theta_{d_i}}(\mathbf{x}_i) \right) \\ &\quad \cdot \left(\sum_{d_{|I|+1} \dots d_N=1}^M \mathcal{C}_{d_{|I|+1} \dots d_N}^\nu \prod_{i=|I|+1}^N f_{\theta_{d_i}}(\mathbf{x}_i) \right) \end{aligned} \quad (11)$$

For every $\nu \in [R]$, define the functions $g_\nu : (\mathbb{R}^s)^{|I|} \rightarrow \mathbb{R}$ and $g'_\nu : (\mathbb{R}^s)^{|J|} \rightarrow \mathbb{R}$ as follows:

$$\begin{aligned} g_\nu(\mathbf{x}_1, \dots, \mathbf{x}_{|I|}) &:= \sum_{d_1 \dots d_{|I|}=1}^M \mathcal{B}_{d_1 \dots d_{|I|}}^\nu \prod_{i=1}^{|I|} f_{\theta_{d_i}}(\mathbf{x}_i) \\ g'_\nu(\mathbf{x}_1, \dots, \mathbf{x}_{|J|}) &:= \sum_{d_1 \dots d_{|J|}=1}^M \mathcal{C}_{d_1 \dots d_{|J|}}^\nu \prod_{i=1}^{|J|} f_{\theta_{d_i}}(\mathbf{x}_i) \end{aligned}$$

⁶ To see that this does not limit generality, denote $I = \{i_1, \dots, i_{|I|}\}$ and $J = \{j_1, \dots, j_{|J|}\}$, and define an auxiliary function h'_y by permuting the entries of h_y such that those indexed by I are on the left and those indexed by J on the right, i.e. $h'_y(\mathbf{x}_{i_1}, \dots, \mathbf{x}_{i_{|I|}}, \mathbf{x}_{j_1}, \dots, \mathbf{x}_{j_{|J|}}) = h_y(\mathbf{x}_1, \dots, \mathbf{x}_N)$. Obviously $\text{sep}(h_y; I, J) = \text{sep}(h'_y; I', J')$, where the partition (I', J') is defined by $I' = \{1, \dots, |I|\}$ and $J' = \{|I| + 1, \dots, N\}$. Analogously to the definition of h'_y , let \mathcal{A}'^y be the tensor obtained by permuting the modes of \mathcal{A}^y such that those indexed by I are on the left and those indexed by J on the right, i.e. $\mathcal{A}'^y_{d_{i_1} \dots d_{i_{|I|}} d_{j_1} \dots d_{j_{|J|}}} = \mathcal{A}^y_{d_1 \dots d_N}$. It is not difficult to see that matricizing \mathcal{A}'^y w.r.t. (I', J') is equivalent to matricizing \mathcal{A}^y w.r.t. (I, J) , i.e. $[\mathcal{A}'^y]_{I', J'} = [\mathcal{A}^y]_{I, J}$, and in particular $\text{rank}[\mathcal{A}'^y]_{I', J'} = \text{rank}[\mathcal{A}^y]_{I, J}$. Moreover, since by definition \mathcal{A}^y is a coefficient tensor corresponding to h_y (eq. 2), \mathcal{A}'^y will be a coefficient tensor that corresponds to h'_y . Now, our proof will show that $\text{sep}(h'_y; I', J') = \text{rank}[\mathcal{A}'^y]_{I', J'}$, which, in light of the equalities above, implies $\text{sep}(h_y; I, J) = \text{rank}[\mathcal{A}^y]_{I, J}$, as required.

Substituting these into eq. 11 leads to:

$$h_y(\mathbf{x}_1, \dots, \mathbf{x}_N) = \sum_{\nu=1}^R g_\nu(\mathbf{x}_1, \dots, \mathbf{x}_{|I|}) g'_\nu(\mathbf{x}_{|I|+1}, \dots, \mathbf{x}_N)$$

which by definition of the separation rank (eq. 5), implies $\text{sep}(h_y; I, J) \leq R$. By this we have shown that $\text{sep}(h_y; I, J) \leq \text{rank}[\mathcal{A}^y]_{I,J}$, as required.

For proving the converse inequality, i.e. $\text{sep}(h_y; I, J) \geq \text{rank}[\mathcal{A}^y]_{I,J}$, we rely on basic concepts and results from functional analysis, or more specifically, from the topic of L^2 spaces. While a full introduction to this topic is beyond our scope (the interested reader is referred to [25]), we briefly lay out here the minimal background required in order to follow our proof. For any $n \in \mathbb{N}$, $L^2(\mathbb{R}^n)$ is formally defined as the Hilbert space of Lebesgue measurable square-integrable real functions over \mathbb{R}^n ⁷, equipped with standard (point-wise) addition and scalar multiplication, as well as the inner product defined by integration over point-wise multiplication. For our purposes, $L^2(\mathbb{R}^n)$ may simply be thought of as the (infinite-dimensional) vector space of functions $g : \mathbb{R}^n \rightarrow \mathbb{R}$ satisfying $\int g^2 < \infty$, with inner product defined by $\langle g_1, g_2 \rangle := \int g_1 \cdot g_2$. Our proof will make use of the following basic facts related to L^2 spaces:

Fact 1. *If V is a finite-dimensional subspace of $L^2(\mathbb{R}^n)$, then any $g \in L^2(\mathbb{R}^n)$ may be expressed as $g = p + \delta$, with $p \in V$ and $\delta \in V^\perp$ (i.e. δ is orthogonal to all elements in V). Moreover, such a representation is unique, so in the case where $g \in V$, we necessarily have $p = g$ and $\delta \equiv 0$.*

Fact 2. *If $g \in L^2(\mathbb{R}^n)$, $g' \in L^2(\mathbb{R}^{n'})$, then the function $(\mathbf{x}_1, \mathbf{x}_2) \mapsto g(\mathbf{x}_1) \cdot g'(\mathbf{x}_2)$ belongs to $L^2(\mathbb{R}^n \times \mathbb{R}^{n'})$.*

Fact 3. *Let V and V' be finite-dimensional subspaces of $L^2(\mathbb{R}^n)$ and $L^2(\mathbb{R}^{n'})$ respectively, and define $U \subset L^2(\mathbb{R}^n \times \mathbb{R}^{n'})$ to be the subspace spanned by $\{(\mathbf{x}_1, \mathbf{x}_2) \mapsto p(\mathbf{x}_1) \cdot p'(\mathbf{x}_2) : p \in V, p' \in V'\}$. Given $g \in L^2(\mathbb{R}^n)$, $g' \in L^2(\mathbb{R}^{n'})$, consider the function $(\mathbf{x}_1, \mathbf{x}_2) \mapsto g(\mathbf{x}_1) \cdot g'(\mathbf{x}_2)$ in $L^2(\mathbb{R}^n \times \mathbb{R}^{n'})$. This function belongs to U^\perp if $g \in V^\perp$ or $g' \in V'^\perp$.*

Fact 4. *If $g_1, \dots, g_m \in L^2(\mathbb{R}^n)$ are linearly independent, then for any $k \in \mathbb{N}$, the set of functions $\{(\mathbf{x}_1, \dots, \mathbf{x}_k) \mapsto \prod_{i=1}^k g_{d_i}(\mathbf{x}_i)\}_{d_1 \dots d_k \in [m]}$ is linearly independent in $L^2((\mathbb{R}^n)^k)$.*

To facilitate application of the theory of L^2 spaces, we assume that the network's representation functions – $f_{\theta_1} \dots f_{\theta_M} : \mathbb{R}^s \rightarrow \mathbb{R}$, are members of $L^2(\mathbb{R}^s)$. In particular, we assume them to be square-integrable. This may seem as a limitation at first glance, as for example neural representation functions $f_{\theta_d}(\mathbf{x}) = \sigma(\mathbf{w}_d^\top \mathbf{x} + b_d)$, with parameters $\theta_d = (\mathbf{w}_d, b_d) \in \mathbb{R}^s \times \mathbb{R}$ and sigmoidal activation $\sigma(\cdot)$ ⁸, are not square-integrable. However, since in practice the input to a representation function is bounded (e.g. it represents image patches by holding intensity values), we may view the function as having compact support, which, as long as the function is continuous (holds for all cases of interest), ensures square-integrability. With the assumption $f_{\theta_1} \dots f_{\theta_M} \in L^2(\mathbb{R}^s)$ in place, the expression given in eq. 2 for h_y , along with fact 2 above, imply that $h_y \in L^2((\mathbb{R}^s)^N)$. We thus apply the definition of separation rank (eq. 5) to h_y through the outlook of L^2 spaces. That is to say, $\text{sep}(h_y; I, J)$ is understood to be the minimal non-negative integer R such that there exist $g_1 \dots g_R \in L^2((\mathbb{R}^s)^{|I|})$ and $g'_1 \dots g'_R \in L^2((\mathbb{R}^s)^{|J|})$ for which:

$$h_y(\mathbf{x}_1, \dots, \mathbf{x}_N) = \sum_{\nu=1}^R g_\nu(\mathbf{x}_1, \dots, \mathbf{x}_{|I|}) g'_\nu(\mathbf{x}_{|I|+1}, \dots, \mathbf{x}_N) \quad (12)$$

We would like to show that $\text{sep}(h_y; I, J) \geq \text{rank}[\mathcal{A}^y]_{I,J}$. Our strategy for achieving this will be to start from eq. 12, and derive an expression for $[\mathcal{A}^y]_{I,J}$ comprising a sum of R rank-1 matrices. As an initial step along this path, define the following finite-dimensional subspaces:

$$V := \text{span} \left\{ (\mathbf{x}_1, \dots, \mathbf{x}_{|I|}) \mapsto \prod_{i=1}^{|I|} f_{\theta_{d_i}}(\mathbf{x}_i) \right\}_{d_1 \dots d_{|I|} \in [M]} \subset L^2((\mathbb{R}^s)^{|I|}) \quad (13)$$

$$V' := \text{span} \left\{ (\mathbf{x}_1, \dots, \mathbf{x}_{|J|}) \mapsto \prod_{i=1}^{|J|} f_{\theta_{d_i}}(\mathbf{x}_i) \right\}_{d_1 \dots d_{|J|} \in [M]} \subset L^2((\mathbb{R}^s)^{|J|}) \quad (14)$$

$$U := \text{span} \left\{ (\mathbf{x}_1, \dots, \mathbf{x}_N) \mapsto \prod_{i=1}^N f_{\theta_{d_i}}(\mathbf{x}_i) \right\}_{d_1 \dots d_N \in [M]} \subset L^2((\mathbb{R}^s)^N) \quad (15)$$

Notice that $h_y \in U$ (eq. 2), and that U is the span of products from V and V' , i.e.:

$$U = \text{span}\{(\mathbf{x}_1, \dots, \mathbf{x}_N) \mapsto p(\mathbf{x}_1, \dots, \mathbf{x}_{|I|}) \cdot p'(\mathbf{x}_{|I|+1}, \dots, \mathbf{x}_N) : p \in V, p' \in V'\} \quad (16)$$

Returning to eq. 12, we apply fact 1 to obtain orthogonal decompositions of $g_1 \dots g_R$ w.r.t. V , and of $g'_1 \dots g'_R$ w.r.t. V' . This gives $p_1 \dots p_R \in V$, $\delta_1 \dots \delta_R \in V^\perp$, $p'_1 \dots p'_R \in V'$ and $\delta'_1 \dots \delta'_R \in V'^\perp$, such that $g_\nu = p_\nu + \delta_\nu$ and

⁷ More precisely, elements of the space are equivalence classes of functions, where two functions are considered equivalent if the set in \mathbb{R}^n on which they differ has measure zero.

⁸ σ is sigmoidal if it is monotonic with $\lim_{z \rightarrow -\infty} \sigma(z) = c$ and $\lim_{z \rightarrow +\infty} \sigma(z) = C$ for some $c \neq C$ in \mathbb{R} .

$g'_\nu = p'_\nu + \delta'_\nu$ for every $\nu \in [R]$. Plug this into eq. 12:

$$\begin{aligned}
h_y(\mathbf{x}_1, \dots, \mathbf{x}_N) &= \sum_{\nu=1}^R g_\nu(\mathbf{x}_1, \dots, \mathbf{x}_{|I|}) \cdot g'_\nu(\mathbf{x}_{|I|+1}, \dots, \mathbf{x}_N) \\
&= \sum_{\nu=1}^R (p_\nu(\mathbf{x}_1, \dots, \mathbf{x}_{|I|}) + \delta_\nu(\mathbf{x}_1, \dots, \mathbf{x}_{|I|})) \\
&\quad \cdot (p'_\nu(\mathbf{x}_{|I|+1}, \dots, \mathbf{x}_N) + \delta'_\nu(\mathbf{x}_{|I|+1}, \dots, \mathbf{x}_N)) \\
&= \sum_{\nu=1}^R p_\nu(\mathbf{x}_1, \dots, \mathbf{x}_{|I|}) \cdot p'_\nu(\mathbf{x}_{|I|+1}, \dots, \mathbf{x}_N) \\
&\quad + \sum_{\nu=1}^R p_\nu(\mathbf{x}_1, \dots, \mathbf{x}_{|I|}) \cdot \delta'_\nu(\mathbf{x}_{|I|+1}, \dots, \mathbf{x}_N) \\
&\quad + \sum_{\nu=1}^R \delta_\nu(\mathbf{x}_1, \dots, \mathbf{x}_{|I|}) \cdot p'_\nu(\mathbf{x}_{|I|+1}, \dots, \mathbf{x}_N) \\
&\quad + \sum_{\nu=1}^R \delta_\nu(\mathbf{x}_1, \dots, \mathbf{x}_{|I|}) \cdot \delta'_\nu(\mathbf{x}_{|I|+1}, \dots, \mathbf{x}_N)
\end{aligned}$$

Given that U is the span of products from V and V' (eq. 16), and that $p_\nu \in V, \delta_\nu \in V^\perp, p'_\nu \in V', \delta'_\nu \in V'^\perp$, one readily sees that the first term in the latter expression belongs to U , while, according to fact 3, the second, third and fourth terms are orthogonal to U . We thus obtained an orthogonal decomposition of h_y w.r.t. U . Since h_y is contained in U , the orthogonal component must vanish (fact 1), and we amount at:

$$h_y(\mathbf{x}_1, \dots, \mathbf{x}_N) = \sum_{\nu=1}^R p_\nu(\mathbf{x}_1, \dots, \mathbf{x}_{|I|}) \cdot p'_\nu(\mathbf{x}_{|I|+1}, \dots, \mathbf{x}_N) \quad (17)$$

For every $\nu \in [R]$, let \mathcal{B}^ν and \mathcal{C}^ν be coefficient tensors of p_ν and p'_ν w.r.t. the functions that span V and V' (eq. 13 and 14), respectively. Put formally, \mathcal{B}^ν and \mathcal{C}^ν are tensors of orders $|I|$ and $|J|$ (respectively), with dimension M in each mode, meeting:

$$\begin{aligned}
p_\nu(\mathbf{x}_1, \dots, \mathbf{x}_{|I|}) &= \sum_{d_1 \dots d_{|I|}=1}^M \mathcal{B}_{d_1 \dots d_{|I|}}^\nu \prod_{i=1}^{|I|} f_{\theta_{d_i}}(\mathbf{x}_i) \\
p'_\nu(\mathbf{x}_1, \dots, \mathbf{x}_{|J|}) &= \sum_{d_1 \dots d_{|J|}=1}^M \mathcal{C}_{d_1 \dots d_{|J|}}^\nu \prod_{i=1}^{|J|} f_{\theta_{d_i}}(\mathbf{x}_i)
\end{aligned}$$

Substitute into eq. 17:

$$\begin{aligned}
h_y(\mathbf{x}_1, \dots, \mathbf{x}_N) &= \sum_{\nu=1}^R \left(\sum_{d_1 \dots d_{|I|}=1}^M \mathcal{B}_{d_1 \dots d_{|I|}}^\nu \prod_{i=1}^{|I|} f_{\theta_{d_i}}(\mathbf{x}_i) \right) \\
&\quad \cdot \left(\sum_{d_{|I|+1} \dots d_N=1}^M \mathcal{C}_{d_{|I|+1} \dots d_N}^\nu \prod_{i=|I|+1}^N f_{\theta_{d_i}}(\mathbf{x}_i) \right) \\
&= \sum_{\nu=1}^R \sum_{d_1 \dots d_N=1}^M \mathcal{B}_{d_1 \dots d_{|I|}}^\nu \cdot \mathcal{C}_{d_{|I|+1} \dots d_N}^\nu \prod_{i=1}^N f_{\theta_{d_i}}(\mathbf{x}_i) \\
&= \sum_{d_1 \dots d_N=1}^M \left(\sum_{\nu=1}^R \mathcal{B}_{d_1 \dots d_{|I|}}^\nu \cdot \mathcal{C}_{d_{|I|+1} \dots d_N}^\nu \right) \prod_{i=1}^N f_{\theta_{d_i}}(\mathbf{x}_i)
\end{aligned}$$

Compare this expression for h_y to that given in eq. 2:

$$\sum_{d_1 \dots d_N=1}^M \left(\sum_{\nu=1}^R \mathcal{B}_{d_1 \dots d_{|I|}}^\nu \cdot \mathcal{C}_{d_{|I|+1} \dots d_N}^\nu \right) \prod_{i=1}^N f_{\theta_{d_i}}(\mathbf{x}_i) = \sum_{d_1 \dots d_N=1}^M \mathcal{A}_{d_1, \dots, d_N}^y \prod_{i=1}^N f_{\theta_{d_i}}(\mathbf{x}_i) \quad (18)$$

At this point we utilize the given linear independence of $f_{\theta_1} \dots f_{\theta_M} \in L^2(\mathbb{R}^s)$, from which it follows (fact 4) that the functions spanning U (eq. 15) are linearly independent in $L^2((\mathbb{R}^s)^N)$. Both sides of eq. 18 are linear combinations of these functions, thus their coefficients must coincide:

$$\mathcal{A}_{d_1, \dots, d_N}^y = \sum_{\nu=1}^R \mathcal{B}_{d_1 \dots d_{|I|}}^\nu \cdot \mathcal{C}_{d_{|I|+1} \dots d_N}^\nu, \forall d_1 \dots d_N \in [M] \iff \mathcal{A}^y = \sum_{\nu=1}^R \mathcal{B}^\nu \otimes \mathcal{C}^\nu$$

Matricizing the tensor equation on the right w.r.t. (I, J) gives:

$$\begin{aligned}
\llbracket \mathcal{A}^y \rrbracket_{I, J} &= \llbracket \sum_{\nu=1}^R \mathcal{B}^\nu \otimes \mathcal{C}^\nu \rrbracket_{I, J} \\
&= \sum_{\nu=1}^R \llbracket \mathcal{B}^\nu \otimes \mathcal{C}^\nu \rrbracket_{I, J} \\
&= \sum_{\nu=1}^R \llbracket \mathcal{B}^\nu \rrbracket_{I \cap [|I|], J \cap [|I|]} \odot \llbracket \mathcal{C}^\nu \rrbracket_{(I - |I|) \cap [|J|], (J - |I|) \cap [|J|]} \\
&= \sum_{\nu=1}^R \llbracket \mathcal{B}^\nu \rrbracket_{[|I|], \emptyset} \odot \llbracket \mathcal{C}^\nu \rrbracket_{\emptyset, [|J|]}
\end{aligned}$$

where the second equality is based on the linearity of the matricization operator, the third equality relies on the relation in eq. 1, and the last equality makes use of the assumption $I = \{1, \dots, |I|\}, J = \{|I| + 1, \dots, N\}$.

For every $\nu \in [R]$, $\llbracket \mathcal{B}^\nu \rrbracket_{[I], \emptyset}$ is a column vector of dimension $M^{|I|}$ and $\llbracket \mathcal{C}^\nu \rrbracket_{\emptyset, [J]}$ is a row vector of dimension $M^{|J|}$. Denoting these by \mathbf{u}_ν and \mathbf{v}_ν^\top respectively, we may write:

$$\llbracket \mathcal{A}^y \rrbracket_{I,J} = \sum_{\nu=1}^R \mathbf{u}_\nu \mathbf{v}_\nu^\top$$

This shows that $\text{rank} \llbracket \mathcal{A}^y \rrbracket_{I,J} \leq R$. Since R is a general non-negative integer that admits eq. 12, we may take it to be minimal, i.e. to be equal to $\text{sep}(h_y; I, J)$ – the separation rank of h_y w.r.t. (I, J) . By this we obtain $\text{rank} \llbracket \mathcal{A}^y \rrbracket_{I,J} \leq \text{sep}(h_y; I, J)$, which is what we set out to prove. \square

A.2 Proof of claim 2

The claim is framed in measure theoretical terms, and in accordance, so will its proof be. While a complete introduction to measure theory is beyond our scope (the interested reader is referred to [15]), we briefly convey here the intuition behind the concepts we will be using, as well as facts we rely upon. The *Lebesgue measure* is defined over sets in a Euclidean space, and may be interpreted as quantifying their “volumes”. For example, the Lebesgue measure of a hypercube is one, of the entire space is infinity, and of a finite set of points is zero. In this context, when a phenomenon is said to occur *almost everywhere*, it means that the set of points in which it does not occur has Lebesgue measure zero, i.e. is negligible. An important result we will make use of (proven in [4] for example) is the following. Given a polynomial defined over n real variables, the set of points in \mathbb{R}^n on which it vanishes is either the entire space (when the polynomial in question is the zero polynomial), or it must have Lebesgue measure zero. In other words, if a polynomial is not identically zero, it must be different from zero almost everywhere.

Heading on to the proof, we recall from sec. 3 that the entries of the coefficient tensor \mathcal{A}^y (eq. 2) are given by polynomials in the network’s conv weights $\{\mathbf{a}^{l,\gamma}\}_{l,\gamma}$ and output weights $\mathbf{a}^{L,y}$. Since $\llbracket \mathcal{A}^y \rrbracket_{I,J}$ – the matricization of \mathcal{A}^y w.r.t. the partition (I, J) , is merely a rearrangement of the tensor as a matrix, this matrix too will have entries given by polynomials in the network’s linear weights. Now, denote by r the maximal rank taken by $\llbracket \mathcal{A}^y \rrbracket_{I,J}$ as network weights vary, and consider a specific setting of weights for which this rank is attained. We may assume without loss of generality that under this setting, the top-left r -by- r block of $\llbracket \mathcal{A}^y \rrbracket_{I,J}$ is non-singular. The corresponding minor, i.e. the determinant of the sub-matrix $(\llbracket \mathcal{A}^y \rrbracket_{I,J})_{1:r, 1:r}$, is thus a polynomial defined over $\{\mathbf{a}^{l,\gamma}\}_{l,\gamma}$ and $\mathbf{a}^{L,y}$ which is not identically zero. In light of the above, this polynomial is different from zero almost everywhere, implying that $\text{rank}(\llbracket \mathcal{A}^y \rrbracket_{I,J})_{1:r, 1:r} = r$ almost everywhere. Since $\text{rank} \llbracket \mathcal{A}^y \rrbracket_{I,J} \geq \text{rank}(\llbracket \mathcal{A}^y \rrbracket_{I,J})_{1:r, 1:r}$, and since by definition r is the maximal rank that $\llbracket \mathcal{A}^y \rrbracket_{I,J}$ can take, we have that $\text{rank} \llbracket \mathcal{A}^y \rrbracket_{I,J}$ is maximal almost everywhere. \square

A.3 Proof of theorem 1

The matrix decomposition in eq. 7 expresses $\llbracket \mathcal{A} \rrbracket_{I,J}$ in terms of the network’s linear weights – $\{\mathbf{a}^{0,\gamma} \in \mathbb{R}^M\}_{\gamma \in [r_0]}$ for conv operator in hidden layer 0, $\{\mathbf{a}^{l,\gamma} \in \mathbb{R}^{r_{l-1}}\}_{\gamma \in [r_l]}$ for conv operator in hidden layer $l = 1 \dots L-1$, and $\mathbf{a}^{L,y} \in \mathbb{R}^{r_{L-1}}$ for node y of dense output operator. We prove lower and upper bounds on the maximal rank that $\llbracket \mathcal{A} \rrbracket_{I,J}$ can take as these weights vary. Our proof relies on the rank-multiplicative property of the Kronecker product ($\text{rank}(A \odot B) = \text{rank}(A) \cdot \text{rank}(B)$ for any real matrices A and B – see [1] for proof), but is otherwise elementary.

Beginning with the lower bound, consider the following weight setting (\mathbf{e}_γ here stands for a vector holding 1 in entry γ and 0 at all other entries, $\mathbf{0}$ stands for a vector holding 0 at all entries, and $\mathbf{1}$ stands for a vector holding 1 at all entries, with the dimension of a vector to be understood by context):

$$\begin{aligned} \mathbf{a}^{0,\gamma} &= \begin{cases} \mathbf{e}_\gamma & , \gamma \leq \min\{r_0, M\} \\ \mathbf{0} & , \text{otherwise} \end{cases} \\ \mathbf{a}^{1,\gamma} &= \begin{cases} \mathbf{1} & , \gamma = 1 \\ \mathbf{0} & , \text{otherwise} \end{cases} \\ \mathbf{a}^{l,\gamma} &= \begin{cases} \mathbf{e}_1 & , \gamma = 1 \\ \mathbf{0} & , \text{otherwise} \end{cases} \quad \text{for } l = 2 \dots L-1 \\ \mathbf{a}^{L,y} &= \mathbf{e}_1 \end{aligned} \tag{19}$$

Let $n \in [N/4]$. Recalling the definition of $I_{l,k}$ and $J_{l,k}$ from eq. 6, consider the sets $I_{1,n}$ and $J_{1,n}$, as well as $I_{0,4(n-1)+t}$ and $J_{0,4(n-1)+t}$ for $t \in [4]$. $(I_{1,n}, J_{1,n})$ is a partition of $[4]$, i.e. $I_{1,n} \cup J_{1,n} = [4]$, and for every $t \in [4]$ we have $I_{0,4(n-1)+t} = \{1\}$ and $J_{0,4(n-1)+t} = \emptyset$ if t belongs to $I_{1,n}$, and otherwise $I_{0,4(n-1)+t} = \emptyset$ and $J_{0,4(n-1)+t} = \{1\}$ if t belongs to $J_{1,n}$. This implies that for an arbitrary vector \mathbf{v} , the matricization

$\llbracket \mathbf{v} \rrbracket_{I_{0,4(n-1)+t}, J_{0,4(n-1)+t}}$ is equal to \mathbf{v} if $t \in I_{1,n}$, and to \mathbf{v}^\top if $t \in J_{1,n}$. Accordingly, for any $\gamma \in [r_0]$:

$$\bigodot_{t=1}^4 \llbracket \mathbf{a}^{0,\gamma} \rrbracket_{I_{0,4(n-1)+t}, J_{0,4(n-1)+t}} = \begin{cases} (\mathbf{a}^{0,\gamma} \odot \mathbf{a}^{0,\gamma} \odot \mathbf{a}^{0,\gamma} \odot \mathbf{a}^{0,\gamma})^\top, & |I_{1,n}| = 4 \mid |J_{1,n}| = 0 \\ (\mathbf{a}^{0,\gamma} \odot \mathbf{a}^{0,\gamma} \odot \mathbf{a}^{0,\gamma})(\mathbf{a}^{0,\gamma})^\top, & |I_{1,n}| = 3 \mid |J_{1,n}| = 1 \\ (\mathbf{a}^{0,\gamma} \odot \mathbf{a}^{0,\gamma})(\mathbf{a}^{0,\gamma} \odot \mathbf{a}^{0,\gamma})^\top, & |I_{1,n}| = 2 \mid |J_{1,n}| = 2 \\ (\mathbf{a}^{0,\gamma})(\mathbf{a}^{0,\gamma} \odot \mathbf{a}^{0,\gamma} \odot \mathbf{a}^{0,\gamma})^\top, & |I_{1,n}| = 1 \mid |J_{1,n}| = 3 \\ (\mathbf{a}^{0,\gamma} \odot \mathbf{a}^{0,\gamma} \odot \mathbf{a}^{0,\gamma} \odot \mathbf{a}^{0,\gamma})^\top, & |I_{1,n}| = 0 \mid |J_{1,n}| = 4 \end{cases}$$

Assume that $\gamma \leq \min\{r_0, M\}$. By our setting $\mathbf{a}^{0,\gamma} = \mathbf{e}_\gamma$, so the above matrix holds 1 in a single entry and 0 in all the rest. Moreover, if the matrix is not a row or column vector, *i.e.* if both $I_{1,n}$ and $J_{1,n}$ are non-empty, the column index and row index of the entry holding 1 are both unique w.r.t. γ , *i.e.* they do not repeat as γ ranges over $1 \dots \min\{r_0, M\}$. We thus have:

$$\text{rank} \left(\sum_{\gamma=1}^{\min\{r_0, M\}} \bigodot_{t=1}^4 \llbracket \mathbf{a}^{0,\gamma} \rrbracket_{I_{0,4(n-1)+t}, J_{0,4(n-1)+t}} \right) = \begin{cases} \min\{r_0, M\} & , I_{1,n} \neq \emptyset \wedge J_{1,n} \neq \emptyset \\ 1 & , I_{1,n} = \emptyset \vee J_{1,n} = \emptyset \end{cases}$$

Since we set $\mathbf{a}^{1,1} = \mathbf{1}$ and $\mathbf{a}^{0,\gamma} = \mathbf{0}$ for $\gamma > \min\{r_0, M\}$, we may write:

$$\text{rank} \left(\sum_{\gamma=1}^{r_0} a_\gamma^{1,1} \cdot \bigodot_{t=1}^4 \llbracket \mathbf{a}^{0,\gamma} \rrbracket_{I_{0,4(n-1)+t}, J_{0,4(n-1)+t}} \right) = \begin{cases} \min\{r_0, M\} & , I_{1,n} \neq \emptyset \wedge J_{1,n} \neq \emptyset \\ 1 & , I_{1,n} = \emptyset \vee J_{1,n} = \emptyset \end{cases}$$

The latter matrix is by definition equal to $\llbracket \phi^{1,1} \rrbracket_{I_{1,n}, J_{1,n}}$ (see top row of eq. 7), and so for every $n \in [N/4]$:

$$\text{rank} \llbracket \phi^{1,1} \rrbracket_{I_{1,n}, J_{1,n}} = \begin{cases} \min\{r_0, M\} & , I_{1,n} \neq \emptyset \wedge J_{1,n} \neq \emptyset \\ 1 & , I_{1,n} = \emptyset \vee J_{1,n} = \emptyset \end{cases} \quad (20)$$

Now, the fact that we set $\mathbf{a}^{L,y} = \mathbf{e}_1$ and $\mathbf{a}^{l,1} = \mathbf{e}_1$ for $l = 2 \dots L-1$, implies that the second to last levels of the decomposition in eq. 7 collapse to:

$$\llbracket \mathcal{A}^y \rrbracket_{I,J} = \bigodot_{t=1}^{N/4} \llbracket \phi^{1,1} \rrbracket_{I_{1,t}, J_{1,t}}$$

Applying the rank-multiplicative property of the Kronecker product, and plugging in eq. 20, we obtain:

$$\text{rank} \llbracket \mathcal{A}^y \rrbracket_{I,J} = \prod_{t=1}^{N/4} \text{rank} \llbracket \phi^{1,1} \rrbracket_{I_{1,t}, J_{1,t}} = \min\{r_0, M\}^S$$

where $S := |\{t \in [N/4] : I_{1,t} \neq \emptyset \wedge J_{1,t} \neq \emptyset\}|$. This equality holds for the specific weight setting we defined in eq. 19. Maximizing over all weight settings gives the sought after lower bound:

$$\max_{\{\mathbf{a}^{l,\gamma}\}_{l,\gamma}, \mathbf{a}^{L,y}} \text{rank} \llbracket \mathcal{A}^y \rrbracket_{I,J} \geq \min\{r_0, M\}^S$$

Moving on to the upper bound, we show by induction over $l = 1 \dots L-1$ that for any $k \in [N/4^l]$ and $\gamma \in [r_l]$, the rank of $\llbracket \phi^{l,\gamma} \rrbracket_{I_{l,k}, J_{l,k}}$ is no greater than $c^{l,k}$, regardless of the chosen weight setting. For the base case $l = 1$ we have:

$$\llbracket \phi^{1,\gamma} \rrbracket_{I_{1,k}, J_{1,k}} = \sum_{\alpha=1}^{r_0} a_\alpha^{1,\gamma} \cdot \bigodot_{t=1}^4 \llbracket \mathbf{a}^{0,\alpha} \rrbracket_{I_{0,4(k-1)+t}, J_{0,4(k-1)+t}}$$

The $M^{|I_{1,k}|}$ -by- $M^{|J_{1,k}|}$ matrix $\llbracket \phi^{1,\gamma} \rrbracket_{I_{1,k}, J_{1,k}}$ is given here as a sum of r_0 rank-1 terms, thus obviously its rank is no greater than $\min\{M^{\min\{|I_{1,k}|, |J_{1,k}|\}}, r_0\}$. Since by definition $c^{0,t} = 1$ for all $t \in [N]$, we may write:

$$\text{rank} \llbracket \phi^{1,\gamma} \rrbracket_{I_{1,k}, J_{1,k}} \leq \min \left\{ M^{\min\{|I_{1,k}|, |J_{1,k}|\}}, r_0 \prod_{t=1}^4 c^{0,4(k-1)+t} \right\}$$

$c^{1,k}$ is defined by the right hand side of this inequality, so our inductive hypotheses holds for $l = 1$. For $l > 1$:

$$\llbracket \phi^{l,\gamma} \rrbracket_{I_{l,k}, J_{l,k}} = \sum_{\alpha=1}^{r_{l-1}} a_\alpha^{l,\gamma} \cdot \bigodot_{t=1}^4 \llbracket \phi^{l-1,\alpha} \rrbracket_{I_{l-1,4(k-1)+t}, J_{l-1,4(k-1)+t}}$$

Taking ranks:

$$\begin{aligned} \text{rank} \llbracket \phi^{l,\gamma} \rrbracket_{I_{l,k}, J_{l,k}} &= \text{rank} \left(\sum_{\alpha=1}^{r_{l-1}} a_\alpha^{l,\gamma} \cdot \bigodot_{t=1}^4 \llbracket \phi^{l-1,\alpha} \rrbracket_{I_{l-1,4(k-1)+t}, J_{l-1,4(k-1)+t}} \right) \\ &\leq \sum_{\alpha=1}^{r_{l-1}} \text{rank} \left(\bigodot_{t=1}^4 \llbracket \phi^{l-1,\alpha} \rrbracket_{I_{l-1,4(k-1)+t}, J_{l-1,4(k-1)+t}} \right) \\ &= \sum_{\alpha=1}^{r_{l-1}} \prod_{t=1}^4 \text{rank} \llbracket \phi^{l-1,\alpha} \rrbracket_{I_{l-1,4(k-1)+t}, J_{l-1,4(k-1)+t}} \\ &\leq \sum_{\alpha=1}^{r_{l-1}} \prod_{t=1}^4 c^{l-1,4(k-1)+t} \\ &= r_{l-1} \prod_{t=1}^4 c^{l-1,4(k-1)+t} \end{aligned}$$

where we used rank sub-additivity in the second line, the rank-multiplicative property of the Kronecker product in the third line, and our inductive hypotheses for $l - 1$ in the fourth line. Since the number rows and columns in $\llbracket \phi^{l,\gamma} \rrbracket_{I_l,k,J_l,k}$ is $M^{|I_l,k|}$ and $M^{|J_l,k|}$ respectively, we may incorporate these terms into the inequality, obtaining:

$$\text{rank} \llbracket \phi^{l,\gamma} \rrbracket_{I_l,k,J_l,k} \leq \min \left\{ M^{\min\{|I_l,k|, |J_l,k|\}}, r_{l-1} \prod_{t=1}^4 c^{l-1, 4(k-1)+t} \right\}$$

The right hand side here is equal to $c^{l,k}$ by definition, so our inductive hypotheses indeed holds for all $l = 1 \dots L - 1$. To establish the sought after upper bound on the rank of $\llbracket \mathcal{A}^y \rrbracket_{I,J}$, we recall that the latter is given by:

$$\llbracket \mathcal{A}^y \rrbracket_{I,J} = \sum_{\alpha=1}^{r_{L-1}} a_{\alpha}^{L,y} \cdot \bigodot_{t=1}^4 \llbracket \phi^{L-1,\alpha} \rrbracket_{I_{L-1,t}, J_{L-1,t}}$$

Carrying out a series of steps similar to before, while making use of our inductive hypotheses for $l = L - 1$:

$$\begin{aligned} \text{rank} \llbracket \mathcal{A}^y \rrbracket_{I,J} &= \text{rank} \left(\sum_{\alpha=1}^{r_{L-1}} a_{\alpha}^{L,y} \cdot \bigodot_{t=1}^4 \llbracket \phi^{L-1,\alpha} \rrbracket_{I_{L-1,t}, J_{L-1,t}} \right) \\ &\leq \sum_{\alpha=1}^{r_{L-1}} \text{rank} \left(\bigodot_{t=1}^4 \llbracket \phi^{L-1,\alpha} \rrbracket_{I_{L-1,t}, J_{L-1,t}} \right) \\ &= \sum_{\alpha=1}^{r_{L-1}} \prod_{t=1}^4 \text{rank} \llbracket \phi^{L-1,\alpha} \rrbracket_{I_{L-1,t}, J_{L-1,t}} \\ &\leq \sum_{\alpha=1}^{r_{L-1}} \prod_{t=1}^4 c^{L-1,t} \\ &= r_{L-1} \prod_{t=1}^4 c^{L-1,t} \end{aligned}$$

Since $\llbracket \mathcal{A}^y \rrbracket_{I,J}$ has $M^{|I|}$ rows and $M^{|J|}$ columns, we may include these terms in the inequality, thus reaching the upper bound we set out to prove. □